

The H I Mass Function of Galaxies from a Deep Survey in the 21cm Line

Martin A. Zwaan, Frank H. Briggs, and David Sprayberry

Kapteyn Astronomical Institute, Postbus 800, 9700 AV Groningen, The Netherlands;
zwaan@astro.rug.nl, fbriggs@astro.rug.nl, dspray@astro.rug.nl

and

Ertu Sorar¹

Department of Physics & Astronomy, University of Pittsburgh, Pittsburgh, PA 15260

ABSTRACT

The H I mass function (HiMF) for galaxies in the local universe is constructed from the results of the Arecibo H I Strip Survey, a blind extragalactic survey in the 21cm line. The survey consists of two strips covering in total ~ 65 square degrees of sky, with a depth of $cz = 7400 \text{ km s}^{-1}$ and was optimized to detect column densities of neutral gas $N_{\text{HI}} > 10^{18} \text{ cm}^{-2}$ (5σ). The survey yielded 66 significant extragalactic signals of which approximately 50% are cataloged galaxies. No free floating H I clouds without stars are found. VLA follow-up observations of all signals have been used to obtain better measurements of the positions and fluxes and allow an alternate determination of the achieved survey sensitivity. The resulting HiMF has a shallow faint end slope ($\alpha \approx 1.2$), and is consistent with earlier estimates computed for the population of optically selected gas rich galaxies. This implies that there is not a large population of gas rich low luminosity or low surface brightness galaxies that has gone unnoticed by optical surveys. The influence of large scale structure on the determination of the HiMF from the Arecibo H I Strip Survey is tested by numerical experiments and was not found to affect the resulting HiMF significantly. The cosmological mass density of H I at the present time determined from the survey, $\Omega_{\text{HI}}(z = 0) = (2.0 \pm 0.5) \times 10^{-4} h^{-1}$, is in good agreement with earlier estimates. We determine lower limits to the average

¹current address: QUALCOMM Inc., 6455 Lusk Blvd., San Diego, CA 92121

column densities $\langle N_{\text{HI}} \rangle$ of the galaxies detected in the survey and find that none of the galaxies have $\langle N_{\text{HI}} \rangle < 10^{19.7} \text{cm}^{-2}$, although there are no observational selection criteria against finding lower density systems. Eight percent of the signals detected in the original survey originated in groups of galaxies, whose signals chanced to coincide in frequency.

Subject headings: galaxies: luminosity function, mass function – ISM – surveys
– radio lines: galaxies — galaxies: ISM

1. Introduction

The distribution function of neutral hydrogen masses among galaxies and intergalactic clouds (the H I mass function or HiMF), and more generally, the neutral hydrogen density in the nearby universe, Ω_{HI} , are important inputs into models of cosmology and galaxy evolution. Different attempts have been made to construct an HiMF by using optically selected galaxies (Rao & Briggs 1993, hereafter RB, Solanes, Giovanelli & Haynes 1996). These studies are based on the assumption that H I is always associated with optically bright galaxies. A major concern is whether the HiMF is complete when it is computed for these galaxies.

For example, the population of low surface brightness (LSB) galaxies might hypothetically constitute a substantial portion of the population of nearby extragalactic objects (Disney 1976, McGaugh 1996, Dalcanton, Spergel & Summers 1997, Sprayberry et al. 1997). The LSB population easily escapes detection optically and would not be included in the samples that are commonly used to evaluate the HiMF. This would be particularly problematic since LSB galaxies are generally found to be rich in neutral gas (Schombert et al. 1992, de Blok, McGaugh & van der Hulst 1996) and could therefore contribute substantially to the neutral gas content. Gas rich dwarf galaxies may also play an important part. For example Tyson & Scalo (1988) have argued that the majority of these dwarf galaxies remain undetected because only the small portion that is currently undergoing a rapid phase of star formation is presently observed with optical telescopes. A final possible population of gas rich systems that would escape inclusion in optical catalogs is a class of intergalactic H I clouds without stars. So far, only a few such systems have been discovered, and they are always found to be gravitationally bound to a galaxy or a group of galaxies (for example the Leo ring, Schneider 1989).

Clearly, the HiMF and the H I content of the local universe should be measured directly, in such a way that they suffer no bias against gas rich galaxies or intergalactic H I clouds which are difficult to detect optically. This is possible by means of surveys in the H I line. Several of these surveys have been carried out over the last two decades. The majority were single dish observations using on/off techniques, since these surveys were done in conjunction with observations targeted on cataloged galaxies (Fisher & Tully 1981b, Giovanelli & Haynes 1985, 1989). Some surveys were concentrated on groups of galaxies (Haynes & Roberts 1979, Lo & Sargent 1979, Fisher & Tully 1981a, Hoffman, Lu & Salpeter 1992) to specifically search for H I clouds in the vicinity of known galaxies. Other surveys were designed to find H I signals in voids (Krumm & Brosch 1984, Szomoru et al 1996), or to compare voids and superclusters (Weinberg et al. 1991, Szomoru et al. 1994). Since these surveys are not pointed at randomly chosen regions of sky, they may not provide fair

tests of the shape of the HiMF or an unbiased measure of the average H I density. A few truly blind surveys have been conducted, the first one in driftscan mode (Shostak 1977) and one by observing a series of pointings on lines of constant declination (Kerr & Henning 1987, Henning 1992). It is worrisome that this latter survey could not reproduce the HiMF defined for optically selected galaxies, possibly because the survey was targeted toward large volumes of known voids. Another possibility is that the achieved survey sensitivity is not well understood, leading to an underestimation of the true number density of H I rich galaxies and intergalactic clouds.

More recently, several surveys have been made using the Arecibo telescope (Sorar 1994, Spitzak 1996, Schneider 1997). Surveys are in progress at Dwingeloo (DOGS) and at Parkes, where the survey will cover the entire Southern Sky (Staveley-Smith et al. 1996).

In this paper we analyze the Arecibo H I Strip Survey (Sorar 1994), a blind survey for extragalactic H I covering ~ 65 square degrees of sky, out to a redshift of 7400 km s^{-1} . The analysis of the survey results will concentrate specifically on the understanding of the achieved survey sensitivity and the vulnerability to large scale structure. We describe the details of the survey and the optical and 21cm follow-up observations in section 2. Section 3 gives a detailed analysis of the achieved survey sensitivity. We present the HiMF in section 4, the possible influence of large scale structure on the determination of the HiMF is examined by performing numerical experiments, and the cosmological mass density of H I at the present time is calculated in this section. In section 5 we compare our findings with previous estimates of the HiMF based on 21cm surveys and optically selected galaxy samples and discuss the implications of our results. Section 6 summarizes the results. The distances used in this paper are based on a Hubble constant $H_0 = 100 \text{ km s}^{-1} \text{ Mpc}^{-1}$.

2. Observations

2.1. Arecibo H I Strip Survey (AHiSS)

The strip survey was carried out on the Arecibo² 305m Telescope in the period of August 1993 until February 1994. The survey was designed to take advantage of periods of construction when the telescope pointing was immobilized but the receiving systems were still operational. Therefore, the data were taken in driftscan mode and the telescope beam traced strips of constant declination. The same strips were retraced for as many as

²The Arecibo Observatory is part of the National Astronomy and Ionosphere Center, which is operated by Cornell University under cooperative agreement with the National Science Foundation.

30 days in order to obtain very sensitive observations that are capable of detecting H I of low surface density. The main survey was divided in two sessions: one survey covering 10.5 hours of RA at $\delta = 14^{\circ}14'$, and the second survey covering 9.7 hours of RA at $\delta = 23^{\circ}09'$. All observations were made at night. The limiting column density was 10^{18}cm^{-2} (at a 5σ level) for gas filling the telescope beam, which subtends $3 h^{-1}$ kpc at $3 h^{-1}$ Mpc and $70 h^{-1}$ kpc at $74 h^{-1}$ Mpc. The total sky coverage was approximately 65 square degrees, with a depth of $cz = 7400 \text{ km s}^{-1}$. The survey was capable of detecting H I masses of $6 \times 10^5 h^{-2} M_{\odot}$ at $7 h^{-1}$ Mpc and $1.5 \times 10^8 h^{-2} M_{\odot}$ at the full depth of the survey, in the main beam which has a FWHM of 3 arcmin. The first sidelobe of the telescope beam pattern could detect $1.5 \times 10^9 h^{-2} M_{\odot}$ at the full depth of the survey, which makes the sidelobes effective in detecting high H I mass galaxies over a 15 arcmin wide strip. The details of the AHSS and the data reduction are described by Sorar (1994). A summary of the reduction path is described by Briggs et al. (1997).

The survey yielded a total of 61 detections, of which approximately half could be associated with cataloged galaxies listed in the NASA Extragalactic Database (NED³). Five detections have no obvious counterparts on the Digitized Sky Survey (DSS⁴) although they are more than 10° away from the Galactic plane.

Fig. 1 shows slice diagrams of the location of all H I selected objects compared with galaxies in the CfA catalog (Geller & Huchra 1989). Galaxies within a 10° strip centered on the declination of the strip are plotted. Different symbols are used to distinguish between cataloged (circles) and uncataloged (boxes) galaxies. The size of the symbols reflects the H I mass of the galaxies, in the sense that bigger symbols indicate larger H I masses. The Galactic plane intersects the strips at $\text{RA} \approx 6^{\text{h}}$ and $\text{RA} \approx 19^{\text{h}}$ as indicated by the dashed lines. The CfA catalog is obviously incomplete in these regions of the sky due to Galactic extinction, whereas the H I survey suffers no bias against detection in these regions. It is clear from this figure that H I selected galaxies generally follow the same structures as the optical galaxies. In particular, if we only consider those regions of the sky where the CfA catalog is complete, we find that more than 80% of the H I selected galaxies lie in regions where the average galaxies density is higher than the mean density. This is consistent with

³The NASA/IPAC Extragalactic Database (NED) is operated by the Jet Propulsion Laboratory, California Institute of Technology, under contract with the National Aeronautics and Space Administration.

⁴Based on photographic data of the National Geographic Society – Palomar Observatory Sky Survey (NGS-POSS) obtained using the Oschin Telescope on Palomar Mountain. The NGS-POSS was funded by a grant from the National Geographic Society to the California Institute of Technology. The plates were processed into the present compressed digital form with their permission. The Digitized Sky Survey was produced at the Space Telescope Science Institute under US Government grant NAG W-2166.

the finding that LSB galaxies and gas-rich dwarfs lie on structures delineated by normal, high surface brightness galaxies (Bothun et al. 1986, Thuan, Gott & Schneider 1987, Eder et al. 1989, Thuan et al. 1991, Mo, McGaugh & Bothun 1994). Furthermore, none of the H I selected galaxies in the sections where the CfA is complete are found in regions where the galaxy density is less than one fifth of the cosmic mean. This is in agreement with the results of Szomoru et al. (1994) and Weinberg et al. (1991) that H I selected galaxies are not found in selected void fields. A more detailed analysis of the large scale distribution of the H I selected galaxies will be presented elsewhere.

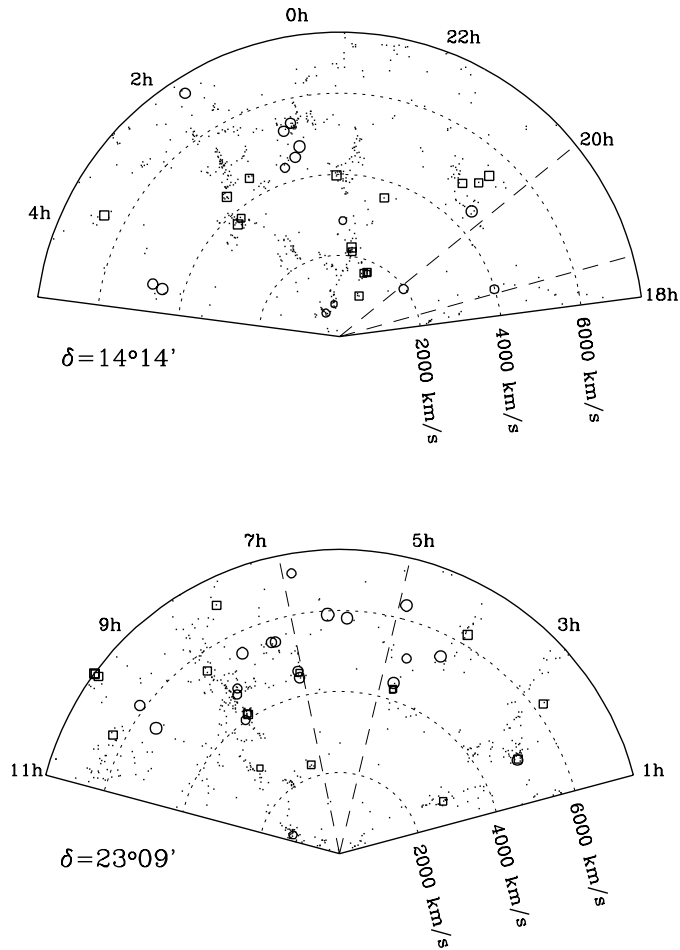


Fig. 1.— Slice diagrams of the location of all the H I selected objects from the Arcicbo H I Strip Survey. Boxes indicate uncataloged galaxies, circles indicate cataloged galaxies. The size of the symbols reflects the H I mass of the galaxies. Also shown are galaxies from the CfA catalog (Geller & Huchra 1989) within a 10° strip centered on the declination of the surveys. The Galactic plane intersects the strips at $RA \approx 6^h$ and $RA \approx 19^h$ as indicated by the dashed lines.

2.2. 21cm Follow-up observations

Follow-up 21cm synthesis observations on all signals found in this survey have been performed with the NRAO⁵ Very Large Array (VLA) in D-configuration. These follow-up observations are essential for three reasons:

- 1) As stated before, the survey was capable of detecting signals as far as 7 arcmin from the center of the survey strip. Consequently, the coordinates yielded by the survey have uncertainties on the order of several arcminutes. The association with a cataloged galaxy or a galaxy on the DSS is therefore not always unambiguous, especially in those cases where there are several prominent galaxies visible within a 15 arcmin wide strip. 21cm observations with spatial resolution of ~ 1 arcmin, are sufficient to obtain unique identifications.
- 2) Flux measurements from the AHiSS can be poor if a signal is detected at large distance from the center of the beam. In principle, a correction to the flux could be made since the response function of the telescope is known with reasonable accuracy, but this is only possible if the positional accuracy is sufficient. Furthermore, measurements from the survey spectra might underestimate the integral flux if the source is more extended than the primary beam. Thus, a rough measure of the H I distribution increases confidence in the analysis.
- 3) Some signals can be caused by pairs or small groups of galaxies, whose line emission might stack up in the same channels. It is not obvious from the Arecibo survey spectra which signals are caused by more than one galaxy. In fact, this situation was found by the VLA observations to occur in five cases.

Short VLA observations (~ 20 min) of all 61 detected galaxies were performed during the D-configuration sessions in May 1995 and September 1996. The signal of three systems fell below the detection limit of the snap-shot observation. These systems were re-observed in the D-configuration during the second session, but with longer integration times (~ 3 hours), resulting finally in confirmation of all 61 detections at levels consistent with the AHiSS sensitivity. The three weaker signals originated in galaxies whose declinations are at the center of the AHiSS.

The VLA observations were performed using 63 channels over a 3.125 MHz bandwidth, corresponding to a velocity range of approximately 660 km s^{-1} . On-line Hanning smoothing was used, resulting in a velocity resolution of $\sim 10.5 \text{ km s}^{-1}$. Phase calibrators were observed once for each source. Only seven different phase calibrators were used. Each time that the phase calibrator was changed, a primary flux calibrator (3C48 or 3C286) was observed in

⁵The National Radio Astronomy Observatory is a facility of the National Science Foundation operated under cooperative agreement by Associated Universities, Inc.

order to tie the flux scales together. Therefore, the primary calibrators were not observed with the same correlator settings as each galaxy, but only with six correlator settings. The overhead time due to slewing of the telescopes and observations of primary calibrators is significantly decreased this way. This technique provided adequate passband calibration for these short observations, where high dynamical range or accurate channel-to-channel flux density calibrations are not needed. There were no strong continuum sources in these fields.

Since the observing conditions were generally quite good, little editing was necessary to remove interference and bad baselines. Continuum was removed from the data in the uv -plane, by making linear fits to the real and imaginary components for each visibility in the line-free channels and subtracting the appropriate values from all channels. The uv data were calibrated and transformed to datacubes using natural weighting. Using natural weighting rather than uniform weighting results in a slightly lower spatial resolution, but higher sensitivity. The resolution in the transformed datacubes is $\sim 60'' \times 60''$. The final r.m.s noise was approximately 1.2 mJy/beam for each channel (corresponding to a minimal detectable column density of $\sim 1.7 \times 10^{19} \text{cm}^{-2}$ [5σ]) for the short integrations and 0.8 mJy/beam (limiting column density $\sim 9 \times 10^{18} \text{cm}^{-2}$ [5σ]) for the longer integrations. Since the observed galaxies were generally barely resolved, CLEANing of the data was not really necessary. Nonetheless, because the synthesized beam of these short observations has strong deviations from a Gaussian shape, we chose to CLEAN the datacubes and restore them with a Gaussian beam in order to make an effective search for companion objects throughout the primary beam.

Total H I masses were calculated using $M_{\text{HI}}/M_{\odot} = 236 d^2 \int S dV$, where d is the distance to the source in Mpc, and S is the flux density in mJy over profile width ΔV in km s^{-1} . Total H I maps were constructed by adding the regions in the channel maps that contain line emission. Contour maps of H I emission and global profiles will be presented in a future paper.

Fig. 2 shows the H I masses as measured with the VLA plotted against the H I masses that are derived from the AHISS spectra. Different symbols are used to distinguish between single detections (filled circles) and multiple detections (open circles). Arecibo measurements of these multiple detections are of course always unreliable estimates of the real H I masses. This figure clearly illustrates the fact that the H I masses derived from the Arecibo spectra generally underestimate the true H I masses, and that follow-up observations were essential to determine accurate measurements. In the analysis of the AHISS results we will use H I masses calculated from the VLA observations, except for galaxies with integrated VLA fluxes less than 1.0 Jy km s^{-1} . Galaxies with these low fluxes are only found at small distances from the center of the Arecibo beam, where the

normalized response function is close to unity. Arecibo measurements for these galaxies are therefore reliable estimates of their real fluxes.

Table 1 summarizes the global parameters of the detected galaxies which are derived from the VLA observations. The following information is contained: Column 1: Identification number of the Arecibo detection. Indices indicate multiple detections. Column 2: Name of galaxy if already cataloged. Columns 3 and 4: B1950 coordinates. Column 5: Logarithm of H I mass. Column 6: Heliocentric velocity, calculated by taking the mean of the velocities at 20% of peak flux density. Column 7: Declination offset from center of the survey strip. Column 8: Identification code for multiple detections.

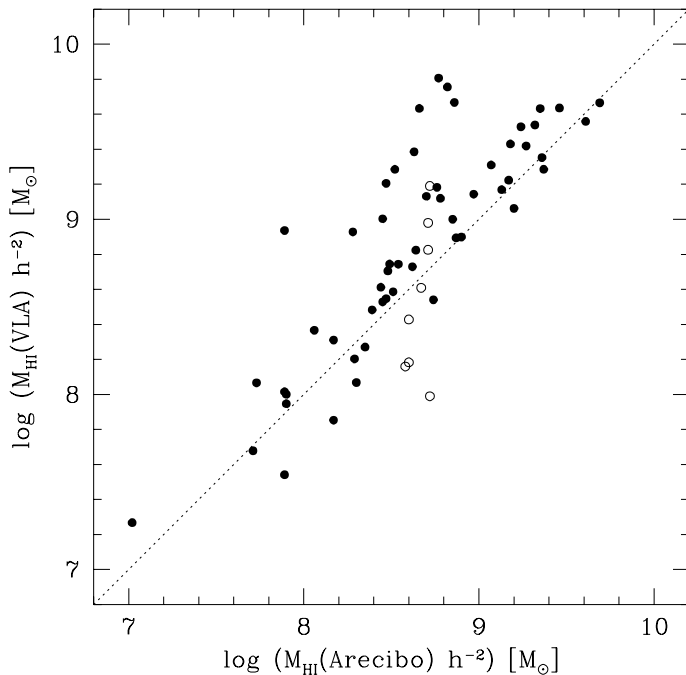


Fig. 2.— Comparison of total H I masses as measured with the VLA and H I masses derived from the Arecibo H I Strip Survey spectra. The dashed line is the line of equality. Different symbols distinguish between single detections (filled circles) and multiple detections (open circles).

2.3. Optical follow-up observations

We have also started a program of optical B -band imaging of the H I selected galaxies with the 2.5m Isaac Newton Telescope⁶ (INT) on La Palma. During four observing runs in the period between October 1995 and March 1997 we have been able to obtain images of all target galaxies. The first noteworthy result of the follow-up optical observations is that *all* of the H I sources more than 10° away from the Galactic plane are found to be associated with galaxies in the B -band images. We have seen no indication that any of the sources detected in the Arecibo survey are anything other than ‘ordinary’ galaxies having both gas and stars. Put another way, we have so far failed to find any H I sources that are pure H I clouds without stars. The analysis of the optical observations will be presented in a subsequent paper.

3. The survey sensitivity

The improved coordinates and H I fluxes derived from the VLA observations help to verify the completeness limit of the survey. The detectability is determined in the following way:

The H I mass in a detected signal can be expressed as $M_{\text{HI}}/M_\odot = 236 \times S \Delta V d^2$, where d is the distance to the source in Mpc, and S is the flux density in mJy that here is considered to be constant over a rectangular profile of width ΔV km/s. The sensitivity of an observation is optimal when the spectra are smoothed to the velocity width of the source. With optimal smoothing the noise becomes $\sigma(\Delta V) = \sigma_0 \sqrt{\Delta V_0/\Delta V}$, where ΔV_0 is the spectral resolution of the receiving system and σ_0 is the noise level in the unsmoothed spectra. The limiting flux density S_c for a 5σ detection is then given by $S_c(\Delta V) = 5\sigma(\Delta V) = 5\sigma_0 \sqrt{\Delta V_0/\Delta V}$. For the AHISS, the average noise level after coadding spectra taken at different days was 0.75 mJy for a velocity resolution of 16 km/s.

The normalized response function of the survey telescope, $I(\theta)$, describes the relative response to a source which is detected at an offset θ from the center of the survey strip. In other words, $I(\theta)$ is the integral of the flux density sensed by the telescope as a source makes a cut through the beam pattern, missing the center of the beam by angle θ , normalized in such a way that $I(0) = 1$. For the Arecibo telescope this function falls off to ~ 0.125 at $\theta = 3.25'$ and reaches a second maximum of ~ 0.2 at $\theta = 4.8'$ due to the high sidelobe level.

⁶The Isaac Newton Telescope is operated by the Royal Greenwich Observatory in the Spanish Observatorio del Roque de los Muchachos of the Instituto Astrofísica de Canarias.

We define a correction factor $c_r(\theta)$ that accounts for the shape of the response function by $c_r(\theta) = 1/I(\theta)$. The limiting flux density of a galaxy at an offset θ from the center of the survey strip can then be expressed as $S_c c_r(\theta)$. In general, an H I source should be detected by the survey if its flux density exceeds this limiting flux density, that is $S > S_c c_r(\theta)$. This can be rewritten as

$$D \equiv \frac{\int S dV \sqrt{(\Delta V_0/\Delta V)}}{5\sigma_0 \Delta V_0 c_f} > c_r(\theta), \quad (1)$$

where we define D as the detectability. The factor c_f represents the normalized feed gain of the telescope, which is a function of frequency. c_f can be approximated by an analytical expression of the form $c_f \approx 1 - ([f - f_0]/w)^2$, where f is the frequency in MHz, f_0 is the center of the survey band and w is a parameter which determines the width of the band. During the observations at $\delta = 14^\circ 14'$ the shape of the normalized feed gain remained unchanged and could be satisfactorily fit by $f_0 = 1395$ MHz and $w = 40.5$ MHz. During the $\delta = 23^\circ 09'$ observations, the gain was retuned a few times to the settings: $f_0 = 1395$ MHz and $w = 37.5$ MHz and $f_0 = 1410$ MHz and $w = 33.8$ MHz. The c_f dependence of D leads to a ‘distance dependence’ for the flux density sensitivity.

The sensitivity can now be verified by plotting the detectability D of the objects against declination offset from the center of the survey strip. This is shown in Fig. 3. All signals that were detected are shown in this plot. The horizontal errorbars are the result of a combination of positional accuracy in the VLA maps and the spatial extent of the galaxies in the direction orthogonal to the survey strip. The signals corresponding to pair or group detections are indicated by open circles and letters A to E are used to identify these related or confused signals in Table 1. Filled circles mark all single object detections. The solid line represents $c_r(\theta)$, the limit to the detectability. In principle, all filled circles should lie above the solid line, the area below this line is ‘undetectable’. The line is a satisfactory limit to the data points, especially if we consider the naive character of Eq.1. That is, this equation assumes that the detected profiles are symmetric and featureless. Since the profiles are generally heavily smoothed, this is a reasonable assumption, but lop-sided profiles or strong double horned profiles might exceed the detection limit while they are formally ‘undetectable’ according to Eq.1.

The limiting depth d_c , the maximum distance to which the object could be placed and still remain within the sample, can now be expressed as a function of M_{HI} , θ and ΔV :

$$d_c(M_{\text{HI}}, \theta, \Delta V) = \sqrt{\frac{M_{\text{HI}} I(\theta)}{236 S_c(\Delta V) \Delta V}}. \quad (2)$$

The variation of feed gain with frequency imposes a minor correction to the limiting

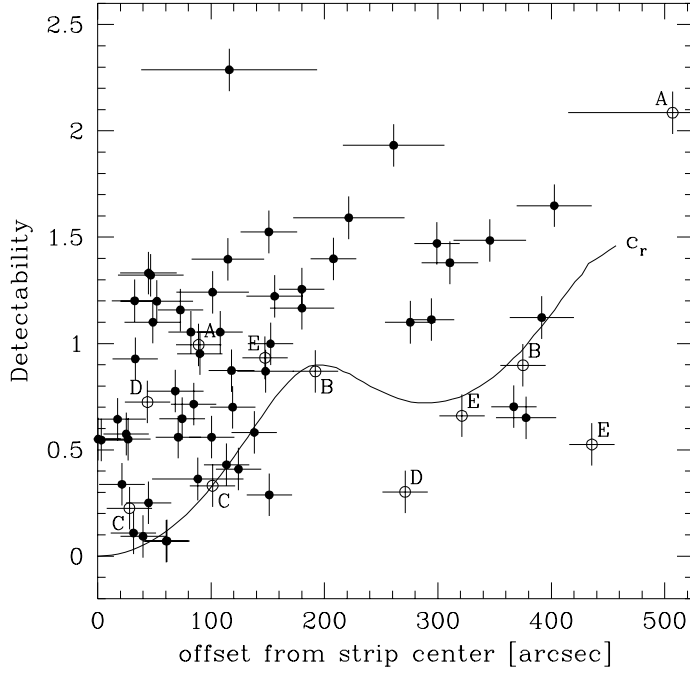


Fig. 3.— Detectability, D , of the objects versus the offset from the center of the survey strip. Multiple detections are indicated by open symbols and coded to indicate which galaxies originate from the same Arecibo detection. The solid curve shows the detection limit. Objects below this line should be undetectable if their H I profile widths would be rectangular.

depth d_c which can be compensated by solving for d_c in

$$S(d_c)c_f(d_c) = S_c, \quad (3)$$

that is, the true flux density $S(d_c)$ of a galaxy located at the distance limit d_c multiplied by the feed gain at a frequency corresponding to that distance has to be equal to the limiting flux density S_c obtained at the center frequency, where the feed gain is optimized and the nominal noise level of the system is normally calculated.

The next step is to calculate the effective search volume of the survey. The volume $d\mathcal{V}$ of a slice of the total survey volume at declination δ and with length l (the total length of the strips in radians, $l = \Delta\text{RA} 2\pi \cos \delta / 24^{\text{h}}$) and width $d\theta$ is given by

$$d\mathcal{V}(M_{\text{HI}}, \theta, \Delta V) = \begin{cases} \frac{1}{3} d_c^3(M_{\text{HI}}, \theta, \Delta V) l d\theta, & \text{if } d_c < d_{\text{BW}}, \\ \frac{1}{3} d_{\text{BW}}^3 l d\theta, & \text{if } d_c > d_{\text{BW}}, \end{cases} \quad (4)$$

where d_{BW} is the limiting depth of the survey imposed by the bandwidth of the receiving system. The total survey volume that is sensitive to a galaxy with H I mass M_{HI} and

velocity spread ΔV can then be calculated by taking the integral over θ . For galaxies in the flux limited regime, for which $d_c < d_{\text{BW}}$ for each θ , this integral simply becomes:

$$\mathcal{V}(M_{\text{HI}}, \Delta V) = \frac{1}{3} \int_{-\infty}^{\infty} d_c^3 l d\theta = \frac{1}{3} \int_{-\infty}^{\infty} \left(\frac{M_{\text{HI}} I(\theta)}{236 S_c \Delta V} \right)^{3/2} l d\theta. \quad (5)$$

For galaxies in the bandwidth limited regime, $d_c > d_{\text{BW}}$ for θ smaller than a certain critical value θ_{BW} . The integral must now be split up in separate parts for the flux limited regimes and the band width limited regime:

$$\begin{aligned} \mathcal{V}(M_{\text{HI}}, \Delta V) &= \frac{1}{3} \int_{-\infty}^{-\theta_{\text{BW}}} d_c^3 l d\theta + \frac{1}{3} \int_{-\theta_{\text{BW}}}^{\theta_{\text{BW}}} d_{\text{BW}}^3 l d\theta + \frac{1}{3} \int_{\theta_{\text{BW}}}^{\infty} d_c^3 l d\theta \\ &= \frac{2}{3} \int_0^{\theta_{\text{BW}}} d_{\text{BW}}^3 l d\theta + \frac{2}{3} \int_{\theta_{\text{BW}}}^{\infty} \left(\frac{M_{\text{HI}} I(\theta)}{236 S_c \Delta V} \right)^{3/2} l d\theta, \end{aligned} \quad (6)$$

where we made use of the symmetry of the beam shape in the last step.

This effective search volume is still dependent on two variables: M_{HI} and ΔV . The most convenient parameterization of \mathcal{V} for computing an HiMF is to express \mathcal{V} as a function of M_{HI} only. This can be achieved by adopting a relation between M_{HI} and ΔV . Such a relation is known to exist since optical luminosity L is related to ΔV via the Tully-Fisher relation (Tully & Fisher 1977), and L is related to M_{HI} as $M_{\text{HI}} \propto L^{0.9}$ (see Briggs 1990). Briggs & Rao (1993, hereafter BR) determined the $M_{\text{HI}}-\Delta V$ relation empirically by plotting ΔV against $\log M_{\text{HI}}$ for 1139 optically selected galaxies from the catalog by Fisher & Tully (1981b). A fit to these points gives $\Delta V = 0.16 M_{\text{HI}}^{1/3}$. Recently, Salpeter & Hoffman (1996) analyzed H I observations of 70 dwarf galaxies and find a similar trend: $\Delta V \propto M_{\text{HI}}^{0.36}$. This relation is therefore valid over a wide range in H I mass. Our data are also in good agreement with this relation. Note that the velocity widths in these relations are not the inclination corrected maximum rotational velocities, but just the observed velocity spreads.

The effective survey volume $\mathcal{V}(M_{\text{HI}})$ can now be calculated by substituting the relation between ΔV and M_{HI} found by BR and $S_c(\Delta V)$ into Eq.5 and Eq.6. This volume as a function of M_{HI} is shown by the solid line in Fig. 4. In the flux limited regime, for H I masses $< 10^{8.5}$, the search volume is $\mathcal{V} \propto M_{\text{HI}}^{5/4}$. (A proportionality often used in the literature is $\mathcal{V} \propto M_{\text{HI}}^{3/2}$ [e.g., Henning 1995, Schneider 1997]. This power 3/2 arises if the dependence of ΔV on M_{HI} is discarded, effectively assuming that all galaxies have the same profile width.) In the high mass region ($M_{\text{HI}} > 10^{9.5}$), the limiting depths are no longer determined by the detectability of the signals, but simply by the bandwidth of the receiving system. Therefore, the effective survey volume for high mass systems is not dependent on H I mass or ΔV . The total survey volume in this regime, is $\sim 3000 h^{-3} \text{Mpc}^3$. For lower H I masses the volume decreases rapidly and is only $\sim 1.0 h^{-3} \text{Mpc}^3$ for $M_{\text{HI}} = 10^7 M_{\odot}$. The

dashed and the dotted line show the effective search volume corresponding to the main beam and the sidelobes, respectively. This figure clearly shows that the sidelobes do not add much volume in the low mass range, but are very effective in finding large H I masses.

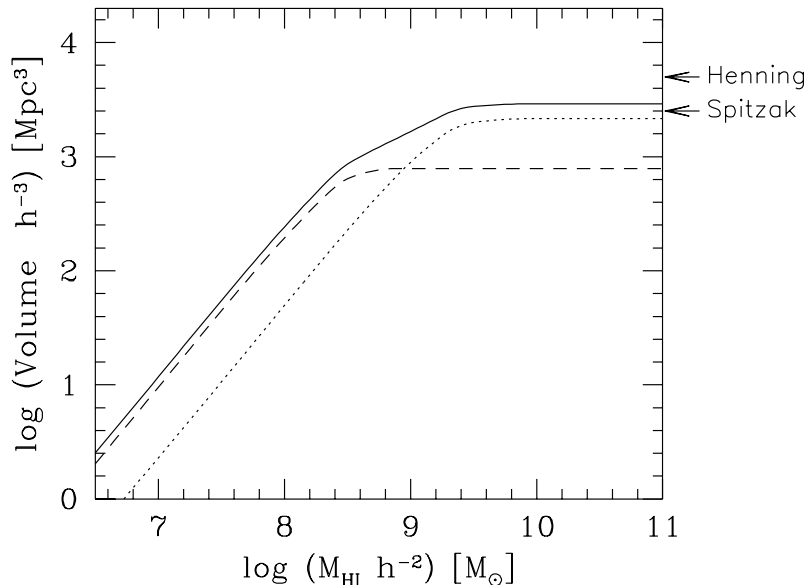


Fig. 4.— The effective search volume vs. H I mass. The solid line is the total search volume of the Arecibo H I Strip Survey, the dashed and the dotted line show the effective search volume corresponding to the main beam and the sidelobes, respectively. The arrows indicate the survey volumes of two H I surveys which are comparable in size to the AHSS: Henning (1995) and Spitzak (1996).

Since the observed velocity width is related to inclination i and maximum rotational velocity V_{\max} as $\Delta V = 2V_{\max} \sin i$, the limiting depth is $d_c \propto (\Delta V)^{-1/4} \propto (\sin i)^{-1/4}$. The limiting depth is therefore weakly dependent on inclination, in the sense that low inclined galaxies can be detected to slightly larger distances. Consequently, an H I survey would in principle preferentially select face-on galaxies. In practice, this effect is negligible, since the expectation for $\langle (\sin i)^{-1/4} \rangle$ of a randomly oriented sample is close to unity:

$$\langle (\sin i)^{-1/4} \rangle = \frac{\int_0^{\pi/2} (\sin i)^{-1/4} \sin i \, di}{\int_0^{\pi/2} \sin i \, di} \approx 1.086. \quad (7)$$

Only the flux limited regime would be hampered by the inclination effect, but most galaxies in this regime are low mass, dwarf galaxies. The velocity spreads are small for these

galaxies, and turbulent motions play an important part at establishing the profile width (cf., Lo, Sargent & Young 1993).

A potential hazard in radio surveys is the influence of radio frequency interference (RFI). RFI can in principle cause false negatives (miss a significant signal) in the sample if it affects the spectrum exactly at the frequency of a source, or when a narrow-lined source is mistaken for RFI. However, the driftscan method that has been used for the AHISS has proven to provide a very good stability for RFI signals (see Briggs et al. 1997). Repetitive coverage of the same regions of sky makes the survey immune to RFI and unstable baselines. This has been demonstrated by the fact that all signals identified in the Arecibo survey have been confirmed by the VLA follow-up.

4. The H I mass function

The H I mass function (HiMF) is defined analogously to optical luminosity functions. The HiMF $\Theta(M_{\text{HI}}/M_{\text{HI}}^*)d(M_{\text{HI}}/M_{\text{HI}}^*)$ gives the total number of galaxies or intergalactic clouds per Mpc^3 in the mass interval $d(M_{\text{HI}}/M_{\text{HI}}^*)$ centered on $M_{\text{HI}}/M_{\text{HI}}^*$. Here, we find it convenient in our analysis and figures to plot the HiMF as the number of galaxies or intergalactic clouds per decade in mass. In order to parameterize the shape of the HiMF, we adopt the conventional Schechter (1976) function,

$$\Theta\left(\frac{M_{\text{HI}}}{M_{\text{HI}}^*}\right)d\left(\frac{M_{\text{HI}}}{M_{\text{HI}}^*}\right) = \theta^*\left(\frac{M_{\text{HI}}}{M_{\text{HI}}^*}\right)^{-\alpha} \exp\left(-\frac{M_{\text{HI}}}{M_{\text{HI}}^*}\right)d\left(\frac{M_{\text{HI}}}{M_{\text{HI}}^*}\right), \quad (8)$$

with free parameters α , the slope of the low-mass end, M_{HI}^* the characteristic mass that defines the kink in the function and θ^* , a normalization factor. This function must be integrated over decade bins for comparison with the binned data in the figures.

4.1. Methods

The classical method (see e.g., Christensen 1975, Schechter 1976) for determining luminosity functions is based on the assumption that galaxies are distributed in a uniform manner. The luminosity function is determined by dividing the number of galaxies in a bin centered on M by $\mathcal{V}(M)$, the effective search volume for that particular M . This method is easily applicable to the AHISS. The search volume can be evaluated with Eq.5 and Eq.6, using a statistical relation between velocity width and H I mass. The advantages of this method are that it is nonparametric and that it is automatically normalized. The important disadvantage is that it assumes homogeneity and its use might lead to errors in $\Theta(M_{\text{HI}})$ if

density fluctuations due to large scale structure occur on distance scales comparable to, or greater than the depth d_c at which M_{HI} can be detected.

A slightly modified form of the ‘classical’ method is the $\sum(1/\mathcal{V}_{\text{max}})$ method, first used by Schmidt (1968), which is also applicable to H I surveys. Instead of calculating a mean survey volume for each mass bin, this method consists of summing the reciprocals of the volumes corresponding to the maximum distances to which the objects could be placed and still remain within the sample. The values of \mathcal{V}_{max} can be calculated directly using Eq.5 and Eq.6, using now the measured velocity spread instead of the statistical value. The two procedures give similar results when the number of galaxies per bin is large. For the less densely populated bins the two procedures can give different results because \mathcal{V}_{max} of a particular galaxy can strongly deviate from the average \mathcal{V} of the mass bin it falls in. In section 4.2 the HiMF is calculated using Schmidt’s method. Like the classical method, Schmidt’s method is also vulnerable to errors caused by large scale structure. The possible effects of large scale structure are discussed in section 4.3.

4.2. Results

Fig. 5 shows the principal results of this analysis. The lower panel shows the observed distribution of H I masses binned per half decade, with errorbars given by Poisson statistics. This histogram shows that the survey has detected galaxies with H I masses in the range from 10^7 to $10^{10}M_{\odot}$ and therefore enables us to determine the HiMF over three orders of magnitudes in H I mass.

The solid dots in the upper panel of Fig. 5 show the HiMF determined by the $\sum(1/\mathcal{V}_{\text{max}})$ method. The errorbars are given by Poisson statistics. Also drawn in this figure are analytical curves given by the Schechter function of Eq 8. A satisfactory fit to the points is obtained with $\alpha = 1.20$, $\theta^* = 0.014 \text{ Mpc}^{-3}$ and $\log(M_{\text{HI}}^*/M_{\odot}) = 9.55$. Mass functions with faint end slopes of 1.10 and 1.30 are shown to indicate the uncertainty in the value of α . We note that in the present analysis the parameterization of the HiMF in the form of a Schechter function is only used to enable comparison with other H I survey results and results based on the optically selected galaxy population. The $\sum(1/\mathcal{V}_{\text{max}})$ method recovers the shape and amplitude of the HiMF simultaneously without using a Schechter function (or any other parameterization) as an assumption about the intrinsic shape of the HiMF.

The observational limits to the determination of the HiMF are also illustrated in Fig. 5 by the thin line. This line represents the sensitivity function of the survey to objects of H I mass M_{HI} , defined as $\phi(M_{\text{HI}}) = 1/\mathcal{V}(M_{\text{HI}})$, where $\mathcal{V}(M_{\text{HI}})$ is the effective search volume.

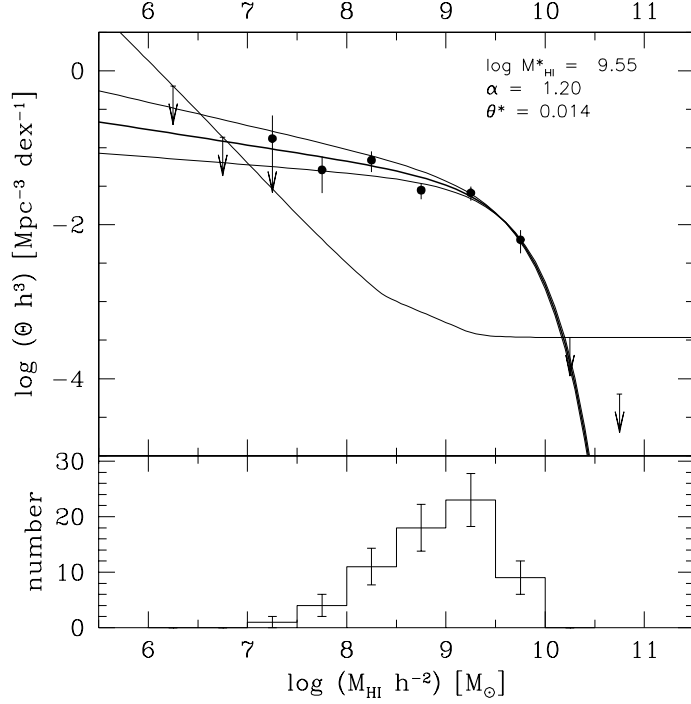


Fig. 5.— Lower panel: The distribution of H I masses of the detected galaxies from VLA follow-up measurements. The errorbars are given by Poisson statistics. Upper panel: The thin line is the sensitivity of the survey defined by $\phi = 1/\mathcal{V}$, where \mathcal{V} is the effective search volume. In the region $10^7 M_\odot < M_{\text{HI}} < 10^{10} M_\odot$ this function defines an upper limit to the space density of intergalactic H I clouds without stars. The measured H I mass function per decade is shown by the points. The fat line is a Schechter luminosity function with parameters as given in the upper right corner. Also Schechter functions with $\alpha = 1.1$ and $\alpha = 1.3$ are shown. The arrows show upper limits to the space density of H I rich galaxies or intergalactic H I clouds. The two arrows on the right are from a complementary survey with the Arecibo telescope over the range 19,000 to 28,000 km s^{-1} .

In the range $10^7 M_\odot < M_{\text{HI}} < 10^{10} M_\odot$ this function defines an upper limit to the space density of intergalactic H I clouds without stars. It also shows that this survey is not capable of measuring the HiMF directly in the regions $M_{\text{HI}} < 10^7 M_\odot$ and $M_{\text{HI}} > 10^{10} M_\odot$ if the extrapolation of the analytical form for $\Theta(M_{\text{HI}})$ holds. The sensitivity function does allow us to define upper limits in these ranges as indicated by arrows. The upper limit at $M_{\text{HI}} = 10^{10.75} M_\odot$ is from the complementary survey with the Arecibo telescope over the range 19,000 to 28,000 km s^{-1} , only sensitive to high mass galaxies (See Sorar (1994) for details).

4.3. Influence of large scale structure

The slice diagrams in Fig 1 show that the survey strips sample a wide range of large scale structure, as the combined RA range extends nearly 2/3 of the way around the sky. On the other hand, the limited depth of the survey for small H I masses might cause the low mass end of the HiMF to be affected by local density fluctuations. Therefore, a major concern in the determination of the mass function following Schmidt’s method, is whether homogeneity is a fair assumption. For instance, a local density enhancement would overestimate the number of low mass galaxies or clouds and would give rise to an overestimate of the faint end slope of the mass function. The biases in the shape of the mass function due to large scale structure can be avoided by making use of a maximum likelihood estimator (cf., Efstathiou, Ellis & Peterson 1988, Saunders et al. 1990). If the spatial density distribution of galaxies and intergalactic clouds is given by $N(M_{\text{HI}}, \vec{r})$, then the overall density $\rho(\vec{r})$ and the mass function $\Theta(M_{\text{HI}})$ can be separated as $N(M_{\text{HI}}, \vec{r}) = \rho(\vec{r})\Theta(M_{\text{HI}})$. Maximum likelihood estimators can then be used to solve either for $\Theta(M_{\text{HI}})$ without knowledge of $\rho(\vec{r})$ or solve for $\rho(\vec{r})$ without knowledge of $\Theta(M_{\text{HI}})$.

Although the maximum likelihood method is a powerful procedure for determining optical luminosity functions (Marzke, Geller & Huchra 1994, Lin et al. 1996, Saunders et al. 1990), we chose not to apply it to the AHiSS. The most important problem is that we have to deal with small number statistics. Especially the faint end slope of the mass function is defined by very few galaxies or clouds per bin. Some experimentation with application of the algorithm to small samples such as ours showed that maximum likelihood methods can produce erratic results in these situations. Another complication arises because maximum likelihood methods assume that the shape of the H I mass function is independent of the space density $\rho(\vec{r})$. In practice, high mass galaxies will have a higher statistical weight in the determination of $\rho(\vec{r})$ since they are simply more numerous in our sample. It is questionable whether this space density defined by the high mass galaxies is a fair estimate for the galaxies at the faint end side of the mass function, in the region that is dominated by dwarf and LSB galaxies. Although these galaxies are found to follow the same general large scale structures as the normal HSB galaxies, they preferentially avoid the highest density regions (Mo et al. 1994, Taylor 1996). In principle, the spatial density ρ could be separated into different functions for individual morphological types or different ranges in H I mass, but the limited number of galaxies in our sample does not allow this differentiation.

In order to investigate the effect of large scale structure we have performed numerical experiments. These tests consisted of randomly placing artificial galaxies in a volume with weights given by the HiMF given in Eq.8. A range of HiMF parameters were investigated. The results are illustrated using the derived HiMF parameters from Fig 5: $\theta = 0.014 \text{ Mpc}^{-3}$,

$\log(M_{\text{HI}}^*/M_{\odot}) = 9.55$ and $\alpha = 1.20$. The galaxies have random inclination, and rotational velocity related to H I mass as determined by BR. Galaxies were selected from these volumes in the same manner as the Arecibo H I Strip Survey selects galaxies from the sky.

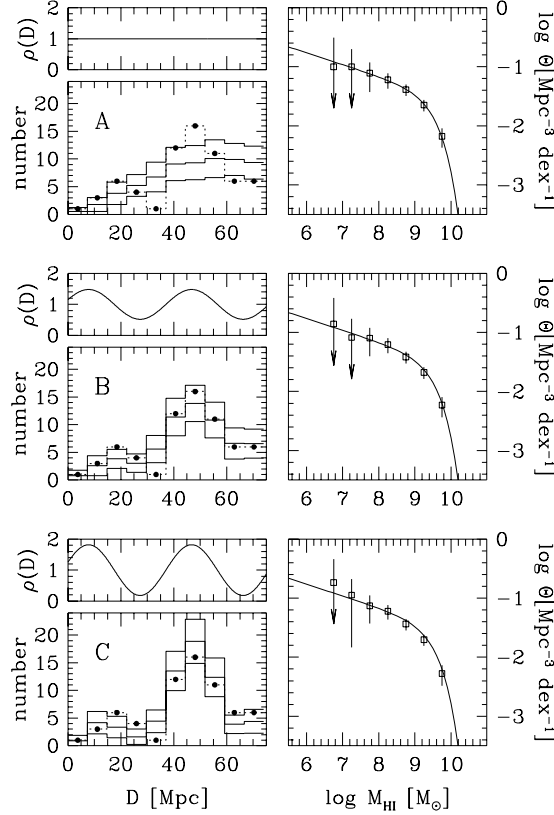


Fig. 6.— Numerical tests of the influence of large scale structure on the determination of the HIIMF. The left panels show the imposed normalized density fluctuations in the artificial catalogs. The histograms show the redshift distributions of the simulated data as solid lines, with 1σ uncertainties as thin lines. The measured redshift distribution of our survey sample is represented by solid circles and a dashed line. The right panels show the $\sum(1/\mathcal{V}_{\text{max}})$ HIIMF of the simulated data as open squares, with 1σ errorbars. The input HIIMF is indicated by the solid curves.

Fig. 6 shows the results of three experiments, labeled as A, B and C. The presented results are each the average of 100 independent simulations. The top panels show the assumed normalized density fluctuations ρ . The central panels show the redshift distribution of the simulated data as thick-lined histograms, thin solid lines show 1σ uncertainties. Overlaid on these histograms is the measured redshift distribution of our survey sample, indicated by solid circles and dashed histograms. The bottom panels show the averaged HIIMFs of the simulated catalogs as open squares, with 1σ errorbars computed as the

standard deviations of the 100 simulations. The $\sum 1/\mathcal{V}_{\max}$ method has been used.

In case A a homogeneous density distribution is assumed. It is not surprising to see that the input HiMF and the measured HiMF agree with high accuracy. The $\sum 1/\mathcal{V}_{\max}$ method should give reliable results in this situation. It is however apparent that the survey observations have several distance bins that are overdense or underdense compared to the uncertainty band of the ‘uniform density’ simulation. The comparison implies that we may be observing underdensities at $D \approx 30$ Mpc and $D \approx 70$ Mpc and an overdensity at $D \approx 50$ Mpc. To test this hypothesis we constructed catalogs with a density fluctuation as indicated by the top panel in case B. The precise functional form of this fluctuation is not important, the condition is that it should produce consecutive under and overdensities at $D \approx 30$, 50 and 70 Mpc. The central panel shows that the imposed density fluctuation reproduces the observed redshift distribution satisfactorily. It is surprising however that if the $\sum 1/\mathcal{V}_{\max}$ method is applied to these simulated data the resulting HiMF is still indistinguishable from the input HiMF. In other words, the $\sum 1/\mathcal{V}_{\max}$ method appears to be a robust method, and not very sensitive to the effects of large scale structure. This is even true for case C, where a more severe density fluctuation is imposed, and where the resulting HiMF is still in good agreement with the input HiMF. We can conclude from these simulations that although we see a hint of the effects of large scale structure in our data, the observed deviations from uniformity have no significant influence on our determination of the HiMF.

5. Discussion

5.1. Previous estimates of the HiMFs from H I surveys

The first H I surveys could only be used to set upper limits to the space density of intergalactic H I clouds without stars, and did not yield enough detections to allow the determination of the shape of the HiMF. Shostak (1977) was the first to define these limits by means of blind driftscan emission and absorption searches in the 21cm line with the NRAO 91m telescope. Due to the relatively poor sensitivity (12 - 40 mJy) and the small total effective search volume ($\sim 300h^{-3}\text{Mpc}^3$), these limits were not very strict. In the region $M_{\text{HI}} < 10^{8.5}M_{\odot}$ the limits set by the Arecibo H I Strip Survey are at least two orders of magnitude lower (99% confidence) than those set by Shostak. Haynes & Roberts (1979), Lo & Sargent (1979) and Fisher & Tully (1981a) search for invisible galaxies in groups of galaxies. Haynes & Roberts conclude from observations in the direction of the Sculptor group that intergalactic H I clouds with $M_{\text{HI}} > 10^8M_{\odot}$ do not exist. Lo & Sargent find four previously uncataloged LSB dwarf galaxies but their upper limits to the space density of unseen objects do not improve Shostak’s. Fisher & Tully used the NRAO 91m telescope to

search for invisible galaxies in the M81 group. Their null result allowed them to push the upper limits to the space density 0.6 dex lower those set by Shostak. Also Krumm & Brosch (1984) find no H I sources in their driftscan searches of void regions and are only able to define upper limits. These limits are not very strict since their survey is only sensitive in the redshift range above 5300 km s^{-1} , and is consequently only capable of finding H I masses $> 10^{10} M_{\odot}$.

A series of papers by Kerr & Henning (1987) and Henning (1992, 1995) describes blind surveys which consisted of observing a series of pointings along lines of constant declination in the zone of avoidance and at high galactic latitude. These surveys yielded 39 detections (of which half were previously unknown) and were the first to put serious constraints on the shape of the HiMF. For comparison, the HiMF calculated by Henning (1995) is reproduced in Fig. 7 as solid squares, together with the AHiSS HiMF represented as a solid line. Henning’s points are significantly lower than our measured curve. According to Henning’s calculations objects with $10^{8.5} M_{\odot} < M_{\text{HI}} < 10^{9.5} M_{\odot}$ are deficient by a one order of magnitude compared to the AHiSS HiMF. The presence of the Local Void in Henning’s survey could explain a part of this discrepancy, but even if the void is omitted the points are still beneath our HiMF. The most reasonable explanation for the discrepancy is that the sensitivity of Henning’s survey is not well understood, leading to a serious underestimate of the HiMF.

The most recent determination of the HiMF is the one by Schneider (1997) who used both the uncorrected Arecibo data from Sorar’s (1994) survey and the data from Spitzak’s (1996) survey with the Arecibo telescope. Schneider assessed the completeness limits of the surveys with the use of $\mathcal{V}/\mathcal{V}_{\text{max}}$ tests. He calculated the average value of $\mathcal{V}/\mathcal{V}_{\text{max}}$ and scaled that to the correct value of 0.5 by increasing the limiting flux density S_c . Schneider noted the vulnerability of this method to the influence of large scale structure. Despite this different approach, the resulting HiMF is in good agreement with our estimate, as can be seen in Fig. 7. Only the low mass end deviates significantly. The statistics in the bins with $M_{\text{HI}} \leq 7.25$ are poor, and Schneider could not rule out a slope as high as $\alpha = 1.7$. The differences in the slopes can be partly explained by the fact that *uncorrected* H I masses are used in Schneider’s estimate of the HiMF from Sorar’s data. The effect that the flux is underestimated when the Arecibo beam misses a galaxy by a certain angle θ was not taken into account. The VLA H I masses that are used in our HiMF are on average 50% higher, leading to a shift of galaxies to higher H I mass bins. As an alternate approach, Schneider also applied a maximum likelihood fit to all the signals brighter than 20σ . The resulting HiMF had a faint end slope $\alpha = 1.32$. This result is also drawn in Fig. 7 and is in very good agreement with our function over the whole range in H I mass.

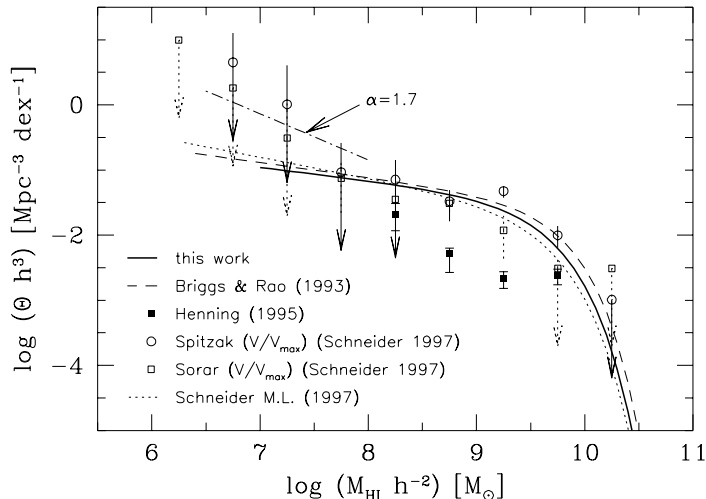


Fig. 7.— Comparison of H I mass functions of different surveys. The fat solid line shows the HiMF presented in this paper, using VLA observations of galaxies found in the Arecibo H I Strip Survey. Briggs & Rao’s (1993) HiMF based on the Fisher & Tully catalog is indicated by dashed curve. The solid squares are from Henning (1995). The open symbols result from Schneider’s (1997) $\mathcal{V}/\mathcal{V}_{\max}$ method applied to the data of Spitzak (1995) (circles) and the uncorrected Arecibo data from Sorar (1994) (squares). Schneider’s (1997) maximum likelihood solution is indicated by the dotted curve. The dash-dot line shows a faint end slope of $\alpha = 1.7$.

In addition to making comparisons with surveys that are equally blind as the AHISS, it is also interesting to compare our results with surveys that cover comparable volumes in underdense and overdense regions. It is noteworthy that the HiMF determined from HI observations in clusters (McMahon 1993), as well as that determined in cosmic voids (Szomoru et al. 1996) are both well fit by a Schechter function, with approximately the same shape as our HiMF. The scaling θ^* , however, differs by a factor of ten or more between these different regions.

Since the AHISS crosses the Galactic plane twice, and consequently a large fraction of the total survey volume lies in regions which are not complete in optical catalogs, it is difficult to calculate the exact void filling factor of our survey. If we limit the calculation to the regions where $|b| > 30^\circ$, we estimate that approximately 50% of the survey volume consists of regions where the average galaxy density is less than one third of the cosmic mean, and approximately 10% of the volume consists of structures where the galaxy density takes on more than three times the cosmic mean. The same percentages are obtained if random slices through the Universe are taken. If voids would be omitted from the survey, the scaling θ^* of the HiMF would increase by a factor of two.

5.2. Comparison with HiMFs bases on optically selected galaxies

The construction of an HiMFs from a sample of optically selected galaxies can either be done statistically, by studying optical luminosity functions and the dependence of H I mass on on optical luminosity, or directly by using 21cm data of optically selected galaxies. The first method was used by RB, who reviewed the literature that describes luminosity functions and H I richness for individual morphological types. Combining these data enabled them to construct an HiMF over three orders of magnitude in H I mass. Their result is in good agreement with our estimate of the HiMF in the range of H I mass where our survey is sensitive.

The second method is discussed by BR who analyzed H I observations drawn from the catalogs of Fisher & Tully (1981b) and Hoffman et al. (1989), and recently by Solanes et al. (1996) who use 21cm data of an optical magnitude-limited sample of galaxies in the direction of the Pisces-Perseus supercluster. Both authors arrive at the same values for the normalization and M_{HI}^* , but their values of the faint end slope differ significantly. BR find $\alpha \sim 1.25$ while Solanes et al. find a declining slope. The Solanes et al. result may not be relevant to the discussion here since their sample excluded all dwarf irregular galaxies and contained no galaxies with $M_{\text{HI}} < 10^{8.5} \sim \frac{1}{10} M_{\text{HI}}^*$. The HiMF determined by BR is reasonably consistent with with our estimate of the HiMF as shown in Fig. 7.

5.3. Implications: A new H I selected galaxy population?

The comparison between our result and the HiMFs based on optically selected galaxy samples provides a direct test of the existence of a new population of gas rich galaxies that has gone unnoticed by optical surveys. In a way, this comparison appraises the completeness of optically selected catalogs for gas rich galaxies. Any contribution of uncataloged gas rich dwarf or gas rich LSB galaxies would yield an difference between HiMFs computed from optically selected and HI-selected galaxy catalogs. Fig 7 shows that the HiMF derived from the results of the AHSS is in very good agreement with previous estimates based on optically selected galaxy catalogs. This implies that the optically selected samples that have been used to evaluate the HiMF are remarkably complete. There is no evidence for a large number of neutral gas rich objects that have escaped inclusion in these catalogs. To the extent that optically selected catalogs are incomplete for LSB galaxies, the excluded galaxies must be predominantly gas poor, consistent with the finding by Sprayberry et al. (1997) that these excluded LSB galaxies are predominantly of low optical luminosity.

Several authors have speculated about the existence of a large class of gas rich dwarf

galaxies (e.g., Dekel & Silk 1986, Tyson & Scalo 1988). These galaxies would yield a steep rise in the HiMF below $M_{\text{HI}} \approx 10^8 M_{\odot}$. We find no observational support for the existence of this class of galaxies. Based on the counting statistics in the mass bins $10^{6.5}$ to $10^8 M_{\odot}$ we can exclude a faint end slope of $\alpha = 1.7$ or steeper with a 99% confidence level.

5.4. Neutral gas density

Our knowledge of Ω_{g} at high redshift is determined by the statistics of Damped Ly- α systems, seen in absorption against background quasars (e.g., Lanzetta, Wolfe & Turnshek 1995, Storrie-Lombardi, Irwin & McMahon 1996). The picture emerging from these studies is that Ω_{g} reaches a maximum at $z \approx 3$ and has been declining since then. At low redshifts different effects complicate the determination of Ω_{g} . Firstly, at redshifts $z < 1.6$, the Ly- α line is not redshifted to optical wavelengths and has to be observed from space (Lanzetta et al. 1995, Rao, Turnshek & Briggs 1995). Secondly, the evaluation of Ω_{g} may depend on the selection effects in the sample of quasars that has been used. Especially at these low redshifts, it is very difficult to compile a unbiased sample of quasars since QSOs would need to be observed within the optical images of galaxies. At the one hand, gravitational lensing can bring faint quasars into the sample which should otherwise be below the detection limit (Smette, Claeskens & Surdej 1997). But on the other hand, dust in Ly- α systems might obscure the background objects to a level where they are undetected (Fall & Pei 1993).

The Arecibo H I Strip Survey can be used to evaluate the gas density differently. The mentioned problems are circumvented since Ω_{g} is not measured by using the Ly- α line, but the 21cm line in emission.

The space density of H I contained in objects of different H I masses is plotted in Fig. 8. The solid line indicates an analytical expression of this function, determined from the product $M_{\text{HI}}\Theta(M_{\text{HI}})$. The thin line represents the sensitivity limits and the arrows mark upper limits determined analogously to the upper limits in Fig 5.

The integral H I mass density at the present epoch can be determined by taking the integral over the solid line in Fig. 8. This yields: $\rho_{\text{HI}} = \Gamma(2 - \alpha)\theta^* M_{\text{HI}}^*$, where Γ is the Euler gamma function. Using the best fit Schechter parameters, we derive that $\rho_{\text{HI}}(z = 0) = 5.8 \times 10^7 h M_{\odot} \text{ Mpc}^{-3}$ or $3.9 \times 10^{-33} h \text{ g cm}^{-3}$, with a statistical error of 20%. A summation over all survey galaxies $\rho_{\text{HI}} = \sum M_{\text{HI}}/\mathcal{V}_{\text{max}}$ yields a slightly smaller value: $\rho_{\text{HI}}(z = 0) = 5.4 \times 10^7 h M_{\odot} \text{ Mpc}^{-3}$ since this calculation does not include the contribution to ρ_{HI} of the density function below $M_{\text{HI}} = 10^7 M_{\odot}$ or above $M_{\text{HI}} = 10^{10} M_{\odot}$. The cosmological mass density of H I at $z = 0$ is $\Omega_{\text{HI}}(z = 0) = (2.1 \pm 0.4) \times 10^{-4} h^{-1}$. The total cosmological

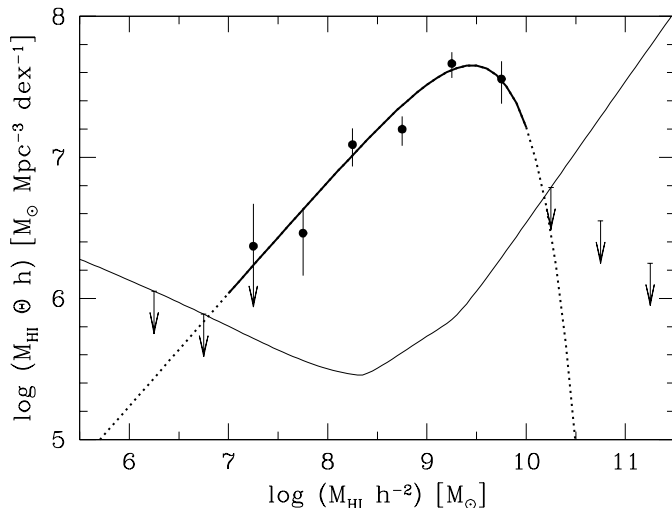


Fig. 8.— Space density of H I mass contained in objects of different masses per decade. The fat line shows the converted analytical H I mass function calculated by multiplying $\Theta \times M_{\text{HI}}$, where Θ is the HiMF plotted in Fig. 5. The dashed regions of the curve indicate that the sample contains no galaxies with $M_{\text{HI}} < 10^7 M_{\odot}$ or $M_{\text{HI}} > 10^{10} M_{\odot}$. The thin line indicates the sensitivity of the survey. The arrows mark upper limits to the space density of H I mass. The three arrows on the right are from a complementary survey with the Arecibo telescope over the range 19,000 to 28,000 km s^{-1} . Note that galaxies with $10^9 M_{\odot} < M_{\text{HI}} < 10^{10} M_{\odot}$ contribute most to the integral H I density.

mass density of neutral gas at the present epoch is $\Omega_{\text{g}}(z = 0) = (2.7 \pm 0.5) \times 10^{-4} h^{-1}$, assuming that the mass percentage of He I is 25% of the total gas density.

This value agrees surprisingly well with earlier estimates by RB, who find $\rho_{\text{HI}}(z = 0) = (4.8 \pm 1.1) \times 10^7 h M_{\odot} \text{ Mpc}^{-3}$ by using optically selected galaxies. Fall & Pei (1993) arrive at approximately the same value of Ω_{HI} by simply computing the average M_{HI}/L_B of the Huchtmeier & Richter (1989) catalog and multiply that by the mean luminosity density in the local universe as estimated by Efstathiou et al. (1988). The agreement between the cosmological mass density based on optically selected galaxies and that based on H I selected galaxies illustrates once more that there is not much neutral gas hidden in objects like LSB galaxies, dwarfs or intergalactic H I clouds that are missed by optical surveys.

The contribution of dwarf galaxies to the H I content of the nearby universe is modest, galaxies with H I masses $< 10^8 M_{\odot}$ make up only $\sim 17\%$ of the integral H I density. The density function in Fig. 8 clearly illustrates that the integral H I mass density is dominated

by high mass galaxies with H I masses in the range $10^9 M_\odot < M_{\text{HI}} < 10^{10} M_\odot$, which are L^* galaxies. At $M_{\text{HI}} \sim 10^{10} M_\odot$ the density function drops off sharply, indicating that Malin 1 type galaxies make no significant contribution to Ω_{HI} . This sharp cutoff was already noted by Bothun (1985). Much stronger upper limits to the contribution of galaxies with $M_{\text{HI}} > 10^{10} M_\odot$ will be set in the near future by the results of the Parkes Multibeam Survey (Staveley-Smith et al. 1996).

The estimate of the integral gas density from the AHISS is a robust result. Two effects cause a relatively low uncertainty in the determination of Ω_{HI} . Firstly, the peak in the H I gas density function is conveniently caused by the galaxies that dominate the counting statistics. Galaxies in the lower mass bins, where the Poisson errors are large, contribute not much to the total density and therefore also not much to the uncertainty in Ω_{HI} . Secondly, the effective search volume in the mass region that dominates the density function is mostly band width limited. Uncertainties in M_{HI} and velocity width do not influence the search volume in this regime.

5.5. What could be missed?

The question arises which gas rich systems could be missed by the survey and could still contribute significantly to the integral gas mass density in the local universe. The only possible candidates that might escape detection are extremely low gas density systems with H I column densities below 10^{18}cm^{-2} , the detection limit of the AHISS.

It has been shown that the gas density of spiral galaxies is correlated with the optical surface brightness in such a way that lower optical surface brightness implies lower gas densities. De Blok et al. (1996) observed a sample of LSB galaxies and showed that the neutral gas densities are generally a factor of two lower than those of late type high surface brightness galaxies. Furthermore, van der Hulst et al. (1993) has shown that the gas densities of LSB galaxies are often just below or equal to the critical density for star formation. If the relation between optical surface brightness and gas density extends to still lower surface brightnesses this implies that galaxies that most easily escape detection in optical surveys are also the ones that might be missed in 21cm surveys.

Until recently, blind H I surveys were not able to reach column densities much lower than 10^{20}cm^{-2} . These surveys would therefore still miss low density systems, and would not be capable to set strict constraints on the number density of LSB galaxies. However, the AHISS is sensitive to column densities $\sim 10^{18} \text{cm}^{-2}$ at a 5σ level for gas filling the beam. Using an extrapolation of the scaling of Disney & Banks (1997),

$N_{\text{HI}} = 10^{20}(M_{\text{HI}}/L_B)10^{0.4(27-\mu_B)}$, where μ_B is the surface brightness averaged over the H I disk, and a typical value of $M_{\text{HI}}/L_B = 1$ for LSB galaxies, the AHISS would be capable of finding galaxies with $\mu_B = 32 \text{ mag arcsec}^{-2}$. Even if a ten times lower value of M_{HI}/L_B is used, and if the area of the galaxy were ten times smaller than the area covered by the Arecibo beam, still galaxies as faint as $\mu_B = 27 \text{ mag arcsec}^{-2}$ would be detectable.

The VLA observations of the AHISS galaxies can be used to set lower limits to average column densities for the sample. Due to the low spatial resolution of the observations ($\sim 1'$), the measured column density is in many cases an average $\langle N_{\text{HI}} \rangle$ over the entire projected surface of the H I layer of the galaxy. If the galaxy is spatially unresolved, an upper limit to the extent D_{HI} of the H I layer can be determined, leading to a lower limit of the average column density $\langle N_{\text{HI}} \rangle \propto M_{\text{HI}}D_{\text{HI}}^{-2}$. Although many of the galaxies in the sample are unresolved, and many of the true values of $\langle N_{\text{HI}} \rangle$ may be higher, we find no values of $\langle N_{\text{HI}} \rangle$ below $10^{19.7} \text{ cm}^{-2}$. Hence, all galaxies in the sample have normal H I column densities, even though there are no observational selection effects against finding extreme low density systems. There is no indication of the existence of a group of extreme low column density galaxies that has been missed by previous H I surveys, simply because they were not capable of reaching the same low column densities as the AHISS. Because we seem to be observing a lower limit to $\langle N_{\text{HI}} \rangle$, much higher than our detection limit, it is very unlikely that galaxies with even lower column densities are missed by the AHISS.

Theoretical predictions of the ionization of gas layers by the extragalactic UV background (Corbelli & Salpeter 1993, Maloney 1993, Charlton, Salpeter & Linder 1994) demonstrate physical mechanisms that can explain the possible non-existence of low column density neutral gas layers. These models predict photoionization by the extragalactic UV background of low column density regions, below $10^{19.5} \text{ cm}^{-2}$. Furthermore, models by Quinn, Katz & Efstathiou (1996) show that the ionization only moderately suppresses the formation of galaxies with rotational speeds larger than 50 km s^{-1} , but that it seriously affects the low density regions around these systems. The models are verified by very deep VLA observations on one galaxy which appears to have a sharp truncation of the HI disk below a column density of $10^{19.5} \text{ cm}^{-2}$ (van Gorkom et al. 1993). Further confirmation of ionization of low density HI comes from recent observations by Bland-Hawthorn et al. (1997) who have detected ionized gas beyond the truncated HI disk in NGC 253.

5.6. H I self absorption

The calculation of the total H I masses in this paper is based on the assumption that the optical depth of the H I layer is close to zero. Any possible influence of H I self

absorption, which will cause an underestimation of the true H I mass, is ignored. In this paragraph we will make a rough estimate of the influence of H I self absorption on the determination of the cosmological mass density Ω_{HI} and the HiMF. The possible effect of self absorption could apply to all HiMFs compared in this paper (see Section 5.1, 5.2 and Fig. 7), since none of these have addressed this possibility.

The problem of self absorption for galaxies can be assessed statistically by plotting the 21cm flux of different Hubble types as a function of inclination i to the line of sight. The line of sight through a inclined galaxy will be larger, generally causing a higher fraction of self absorption. Haynes & Giovanelli (1984) use data of a sample of 1500 galaxies with 21cm fluxes measured with Arecibo. They define a correction factor f_{HI} which is defined by the corrected flux divided by the measured flux and find a general trend: $f_{\text{HI}} = (\cos i)^{-c}$ where c is a constant dependent on morphological type. The values of c are found to be 0.04 for Sa and Sab, 0.16 for Sb and 0.14 for Sbc and Sc galaxies. No correlations are found for morphological types earlier than Sa or later than Sc, indicating that self absorption is negligible in these types. Higher self absorption in types Sb to Sc can be explained by the fact that these galaxies generally have the highest H I surface densities (Cayatte et al. 1994). Furthermore, rotation curves of early type spiral galaxies show the strongest deviations from solid body rotation implying large velocity spreads per line of sight, which further decreases self absorption.

Mean self absorption factors per morphological type can be obtained by averaging f_{HI} over a random distribution of inclinations. This yields

$$\langle f_{\text{HI}} \rangle = \frac{\int_0^{\pi/2} (\cos i)^{-c} \sin i \, di}{\int_0^{\pi/2} \sin i \, di} = 1/(1 - c). \quad (9)$$

The mean correction factors then become 1.04 for Sa and Sab, 1.19 for Sb and 1.16 for Sbc and Sc galaxies.

The cosmological H I mass density is dominated by high mass galaxies, which are statistically most likely to be late type spirals. The correction to Ω_{HI} due to H I self absorption will therefore probably not be more than the value of $\langle f_{\text{HI}} \rangle$ averaged over morphological types Sb to Sd. Assuming that all types Sb to Sd contribute equally to Ω_{HI} , we derive that the mean value of $\langle f_{\text{HI}} \rangle$ is 1.10. Even in the most pessimistic approach, the correction factor can not be more than 1.19.

What will be the effect of H I self absorption on the shape of the HiMF? Using the same arguments as above, we conclude that the effect on the high mass range will be marginal. The normalization factor θ^* and the value which determines the kink, M_{HI}^* , will probably increase by no more than 10%. Galaxies that determine the faint end slope α are

mostly dwarf and LSB galaxies. On the one hand, self absorption may be unimportant because the gas density in these galaxies is usually low (van der Hulst 1993) and the dust content is presumably low (McGaugh 1994) which implies scarcity of clumped gas (Haynes & Giovanelli 1984). On the other hand, the rotation curves of dwarf and LSB galaxies often show solid body rotation (de Blok et al. 1996, Swaters 1997) which causes a low velocity spread along a line of sight, leading to high fractions of self absorption. These two counteracting effects make the value of $\langle f_{\text{HI}} \rangle$ for low mass galaxies uncertain, but probably higher than that for high mass galaxies. After applying the correction factor to the low mass galaxies, some galaxies will shift to higher mass bins, eventually leading to a slightly shallower faint end slope of the mass function. The conclusion that the faint end slope of the mass function is shallow will therefore not be altered by the effects of H I self absorption.

6. Conclusions

We have used the Arecibo H I Strip Survey in combination with 21cm follow-up observations with the VLA to determine the H I mass function of gas rich galaxies in the local universe. The resulting HiMF is in good agreement with earlier estimates based on samples of optically selected galaxies. This implies that there is not a large population of gas rich dwarfs or low surface brightness galaxies, previously undetected by optical surveys. The observed faint end slope of the HiMF is flat ($\alpha \sim 1.2$) leaving no room for a large class of gas rich dwarfs. The cosmological mass density of H I in the local universe is $\Omega_{\text{HI}}(z = 0) = (2.0 \pm 0.5) \times 10^{-4} h^{-1}$, also consistent with earlier estimates. The neutral gas content is dominated by high mass galaxies with $10^9 M_{\odot} < M_{\text{HI}} < 10^{10} M_{\odot}$. The observations indicate the existence of a lower limit to the average H I column density of 19.7 cm^{-2} , consistent with theoretical predictions concerning the ionizing extragalactic UV background.

We thank G. Bothun, E. de Blok, P. Sackett, A. Szomoru, M. Verheijen, and the referee J. van Gorkom for useful comments.

TABLE 1
BASIC PARAMETERS OF SURVEY GALAXIES.

(1) Nr	(2) Name	(3) α (1950) (h m s)	(4) δ (1950) ($^{\circ}$ ' ")	(5) M_{HI} ($\log M_{\odot}$)	(6) V_{\odot} (km/s)	(7) $\Delta\delta$ (")	(8) Code
A1		19:56:40.0	14:07:24	8.02	1964	33	
A2		18:37:52.6	14:11:53	8.32	3991	21	
A3	UGC 11820	21:47:06.0	13:59:50	9.12	1107	116	
A4-1		21:56:41.2	13:59:58	7.99	1720	89	A
A4-2	UGC 11866	21:56:09.0	13:53:00	9.20	1705	507	A
A5		20:23:45.0	14:06:12	9.17	4485	49	
A6	UGC 11611	20:38:11.1	14:05:46	9.64	5412	47	
A7	UGC 11652	20:55:09.1	14:02:58	9.42	4843	52	
A8	UGC 11617	20:41:18.4	14:07:03	9.29	5114	152	
A9	UGC 11921	22:06:49.2	14:06:53	8.82	1672	346	
A10	NGC 7437	22:55:40.9	14:02:28	8.93	2117	151	
A11	UGC 12308	22:58:49.2	14:04:16	9.54	2220	261	
A12		23:23:35.4	13:59:09	7.92	2860	27	
A13	UGC 11992	22:18:20.7	13:58:53	9.31	3591	115	
A14	UGC 12705	23:34:05.2	13:52:48	9.67	3968	403	
A15		00:08:34.1	13:57:45	7.35	812	100	
A16		01:30:19.2	14:07:05	7.68	668	392	
A17		00:17:34.1	14:00:50	9.18	4787	82	
A18		00:21:55.2	13:59:05	8.51	5397	25	
A19		00:25:28.8	14:01:30	8.90	4552	119	
A20		00:30:51.3	13:59:30	8.62	5246	3	
A21		00:41:45.9	14:00:51	8.33	4372	71	
A22	UGC 1087	01:28:46.5	14:01:16	9.35	4484	45	
A23		01:39:44.4	13:59:20	8.79	7103	88	
A24	NGC 820	02:05:42.3	14:06:46	9.56	4418	311	
A25		02:08:50.7	14:00:17	8.62	3794	85	
A26	UGC 1817	02:18:47.5	13:58:22	9.63	3735	222	
A27	UGC 2839	03:41:02.0	14:08:30	9.76	6523	156	
A28		04:27:13.5	14:09:45	8.89	4781	68	
A29		04:30:00.0	14:06:40	9.00	4523	118	
A30	UGC 1294	01:47:26.2	22:54:44	8.71	2861	73	
A31		01:50:57.5	22:53:59	8.97	4956	124	
A32	F 477-01	01:51:46.9	22:57:35	9.13	4989	90	
A33	UGC 1938	02:25:32.1	22:59:20	9.48	6383	108	
A34	UGC 2927	03:58:41.5	22:58:20	9.81	6251	180	
A35		04:11:36.0	23:00:00	9.21	5464	148	
A36		04:44:14.3	23:04:19	8.45	5088	1	
A37-1		04:47:54.5	23:10:50	8.98	4272	375	B
A37-2	UGC 3183	04:48:18.6	23:07:29	8.93	4390	192	B
A38		04:49:52.4	23:05:12	9.22	4416	33	
A39		04:59:39.3	23:10:10	9.43	6339	294	
A40		05:52:39.4	23:02:29	9.06	5812	367	
A41		06:11:31.1	23:04:49	9.63	5902	299	
A42		06:38:58.9	23:12:05	8.38	7012	32	
A43	UGC 3751	07:10:53.4	23:10:05	8.94	2300	208	
A44	CGCG116-001	06:50:06.2	23:11:30	8.11	4575	40	
A45-1		06:51:09.6	23:11:52	8.32	4593	28	C
A45-2		06:51:26.4	23:10:38	8.63	4562	101	C
A46		07:07:27.5	23:13:02	8.90	5457	18	
A47		07:11:33.6	23:14:49	9.00	5473	74	
A48		07:43:23.7	23:12:56	9.22	5491	151	
A49	UGC 4031	07:45:19.9	23:21:51	9.29	6834	378	
A50		08:06:52.0	23:17:47	8.41	4790	61	
A51		08:10:56.9	23:17:44	8.01	4667	60	
A52	UGC 4299	08:13:00.2	23:21:37	9.31	4107	271	D
A53		08:13:29.0	23:17:51	8.61	4143	44	D
A54		08:20:18.6	23:18:29	8.29	4029	60	
A55	UGC 4405	08:23:36.2	23:21:25	9.49	5617	276	
A56	CGCG120-049	08:51:26.8	23:20:55	8.15	2882	114	
A57		10:31:55.5	23:20:54	8.00	1238	101	
A58		09:33:37.4	23:20:03	8.81	6132	45	
A59-1	NGC 2929	09:34:39.3	23:23:18	9.72	7499	148	E
A59-2	NGC 2931	09:34:46.8	23:28:06	9.45	7478	436	E
A59-3	NGC 2930	09:34:40.8	23:26:12	9.26	7376	321	E
A60	UGC 5214	09:42:32.5	23:18:07	9.39	5480	180	
A61	UGC 5498	10:09:16.4	23:19:42	9.14	6306	138	

REFERENCES

- Bland-Hawthorn, J., Freeman, K. C., Quinn, P.J. 1997, ApJ, in press
- Bothun, G. B. 1985, 90, 1982
- Bothun, G. B., Beers, T., Mould, J., Huchra, J. 1986, ApJ, 308, 510
- Briggs, F. H. 1990, AJ, 100, 999
- Briggs, F. H., & Rao, S. 1993, ApJ, 417, 494 (BR)
- Briggs, F. H., Sorar, E., Kraan-Korteweg, R. C., & van Driel, W. 1997, PASA, 14, 37
- Cayatte, V., Kotanyl, C., Balkowski, C., & van Gorkom, J. H. 1994, AJ, 107, 1003
- Charlton, J. C., Salpeter, E. E., & Linder, S. M. 1994, ApJ, 430, L29
- Christensen, C. G. 1975, AJ, 80, 282
- Corbelli, E., Salpeter, E. E. 1993, ApJ, 419, 104
- Dalcanton J. J., Spergel, D. N., & Summers, F. J. 1997, ApJ, 482, 659
- de Blok, W. J. G., McGaugh, S. S., & van der Hulst, J. M. 1996, MNRAS, 283, 18
- Dekel, A., & Silk, J. 1986, ApJ, 303, 39
- Disney, M. J. 1976, Nature, 263, 573
- Disney M. J., & Banks, G. 1997, PASA, 14, 69
- Eder, J. A., Oemler, A. JR., Schombert, J. M., & Dekel, A. 1989, ApJ, 340, 29
- Efstathiou, G., Ellis, R. S., & Peterson, B. A. 1988, MNRAS, 231, 479
- Fall, S. M., & Pei, Y. C. 1993, ApJ, 402, 479
- Fisher, J. R., & Tully, R. B. 1975, A&A, 44, 151
- Fisher, J. R., & Tully, R. B. 1981a, ApJS, 47, 139
- Fisher, J. R., & Tully, R. B. 1981b, ApJL, 243, L23
- Geller, M. J., & Huchra, J. P. 1989, Science, 246, 897
- Giovanelli, R., & Haynes, M. P. 1989, ApJL, 346, L5

- Giovanelli, R., & Haynes, M. P. 1985, *AJ*, 90, 2445
- Haynes, M. P. & Roberts, M. S. 1979, *ApJ*, 227, 767
- Haynes, M. P. & Giovanelli, R. 1984, *AJ*, 89, 758
- Henning, P. A. 1992, *ApJS*, 78, 365
- Henning, P. A. 1995, *ApJ*, 450, 578
- Hoffman, G. L., Lewis, B. M., Helou, G., Salpeter, E. E., & Williams, B. M. 1989, *ApJS*, 69, 65
- Hoffman, G. L., Lu, N. Y., & Salpeter, E. E. 1992, *AJ*, 104, 2086
- Huchtmeier, W. K., & Richter, O. -G. 1989, *A General Catalog of H I Observations of Galaxies: The Reference Catalog* (New York: Springer-Verlag)
- Kerr, F. J., & Henning, P. A. 1987, *ApJ*, 320, L99
- Krumm, N., & Brosch, N. 1984, *AJ*, 89, 1461
- Lanzetta, K. M., Wolfe, A. M., & Turnshek, A. M. 1995, *ApJ*, 440, 435
- Lin, H., Kirshner, R. P., Shectman, S. A., Landy, S.D., Oemler, A., Tucker, D. L., & Schechter, P. L. 1996, 464, 60
- Lo, K. Y., & Sargent, W. L. W. 1979, *ApJ*, 227, 756
- Lo, K. Y., & Sargent, W. L. W., Young, K. 1993, *AJ*, 106, 507
- Maloney, P. 1993, *ApJ*, 414, 41
- Marzke, R. O., Geller, M. J., & Huchra, J. P. 1994, *AJ*, 108, 437
- McGaugh, S. S. 1994, *ApJ*, 426, 135
- McGaugh, S. S. 1996, *MNRAS*, 280, 337
- McMahon, P. M. 1993, Ph.D Thesis, Columbia University
- Mo, H. J., McGaugh, S. S., & Bothun, G. D. 1994, *MNRAS*, 267, 129
- Quinn, T., Katz, N., & Efstathiou, G. 1996, *MNRAS*, 278, L49
- Rao, S., Briggs, F. H. 1993, *ApJ*, 419, 515 (RB)

- Rao, S., Turnshek, A. M., & Briggs, F. H. 1995, *ApJ*, 449, 488
- Salpeter, E. E., & Hoffmann, G. L. 1996, *ApJ*, 465, 595
- Saunders, W., Rowan-Robinson, M., Lawrence, A., Efstathiou, G., Kaiser, N., Ellis, R. S., & Frenk, C. S. 1990, *MNRAS*, 242, 318
- Schechter, P. 1976, *ApJ*, 203, 297
- Schmidt, M. 1968, *ApJ*, 151, 393
- Schneider, S. E. 1989, *ApJ*, 343, 94
- Schneider, S. E. 1997, *PASA*, 14, 99
- Schombert, J. M., Bothun, G. D., Schneider, S. E., & McGaugh, S. S. 1992, *AJ*, 103, 1107
- Shostak, G. S. 1977, *A&A*, 54, 919
- Smette, A., Claeskens, J. -F., & Surdej, J. 1997, *NewA*, 2, 53
- Solanes, J. M., Giovanelli, R., & Haynes, M. 1996, *ApJ*, 461, 609
- Sorar, E. 1994, Ph.D. Thesis, University of Pittsburgh
- Spitzak, J. G. 1996, Ph.D. Thesis, University of Massachusetts
- Sprayberry, D., Impey, C. D., Irwin, M. J., & Bothun, G. D. 1997, *ApJ*, 482, 104
- Staveley-Smith, L., Wilson, W. E., Bird, T. S., Disney, M. J., Ekers, R. D., Freeman, K. C., Haynes, R. F., Sinclair, M. W., Vaile, R. A., Webster, R. L., & Wright, A. E. 1996, *PASA*, 13, 243
- Storrie-Lombardi, L. J., Irwin, M. J., & McMahon, R. G. 1996, *MNRAS*, 282, 1330
- Swaters, R. A., 1997, in preparation
- Szomoru, A., Guhathakurta, P., van Gorkom, J. H., Knapen, J. H., Weinberg, D. H., & Fruchter, A. S. 1994, *AJ*, 108, 491
- Szomoru, A., van Gorkom, J. H., Gregg, M. D., & Strauss, M. A. 1996, *AJ*, 111, 2150
- Taylor, C. L. 1997, *ApJ*, 480, 524
- Thuan, T. X., Gott, J. R., & Schneider, S. E. 1987, *ApJL*, 315, L93

- Thuan, T. X., Alimi, J-M., Gott, J. R., & Schneider, S. E. 1991, *ApJ*, 370, 25
- Tully, R. B., & Fisher, J. R., 1977, *A&A*, 54, 661
- Tyson, N. D., & Scalo, J. M. 1988, *ApJ*, 329, 618
- van der Hulst, J. M., Skillman, E. D., Smith, T. R., Bothun, G. D., McGaugh, S. S., & de Blok, W. J. G. 1993, *AJ*, 106, 548
- van Gorkom, J. H. 1993, in *The Environment and Evolution of Galaxies*, ed. J. M. Shull and H. A. Thronson (Kluwer Academic Publishers), 345
- Weinberg, D. H., Szomoru, A., Guhathakurta, P., & van Gorkom, J. H. 1991, *ApJ*, 372, L13